Dalton Transactions

ROYAL SOCIETY OF CHEMISTRY

PAPER

View Article Online
View Journal | View Issue

Cite this: *Dalton Trans.*, 2023, **52**, 13758

Impact of human serum albumin on Cu^{II} and Zn^{II} complexation by ATSM (diacetyl-bis(*N*4-methyl-thiosemicarbazone)) and a water soluble analogue†

Álvaro Martínez-Camarena, *[a,b] Angélique Sour[b] and Peter Faller [b,c]

The chelator diacetyl-bis(*N*4-methylthiosemicarbazone) (ATSM) and its complexes with Cu^{II} and Zn^{II} are becoming increasingly investigated for medical applications such as PET imaging for anti-tumour therapy and the treatment of amyotrophic lateral sclerosis. However, the solubility in water of both the ligand and the complexes presents certain limitations for *in vitro* studies. Moreover, the stability of the Cu^{II} and Zn^{II} complexes and their metal exchange reaction against the potential biological competitor human serum albumin (HSA) has not been studied in depth. In this work it was observed that the ATSM with an added carboxylic group into the structure increases its solubility in aqueous solutions without altering the coordination mode and the conjugated system of the ligand. The poorly water-soluble Cu^{II}– and Zn^{II}–ATSM complexes were prevented from precipitating due to the binding to HSA. Both HSA and ATSM show a similar thermodynamic affinity for Zn^{II}. Finally, the Cu^{II}-competition experiments with EDTA and the water-soluble ATSM ligands yielded an apparent log K_d at pH 7.4 of about −19. When ATSM was added to Cu^{II}- and Zn^{II}-loaded HSA, withdrawing of Zn^{II} was kinetically favoured, but this metal is slowly substituted by the Cu^{II} afterwards taken from HSA so that this protein could be considered as a source of Cu^{II} for ATSM.

Received 25th July 2023,
Accepted 7th September 2023

DOI: 10.1039/d3dt02380j

rsc.li/dalton

Introduction

Bis-thiosemicarbazones (BTSC) such as ATSM (diacetyl-bis(*N*4-methylthiosemicarbazone)) and its derivatives form a family of compounds that can make strong complexes with a variety of metal ions. Among others, they have been investigated over the last decades for different applications in biology and medicine. In particular, research on Cu^{II}–BTSC is highly active for applications as positron emission tomography (PET) agents for imaging,[1–3] as well as for anticancer[4] or antimicrobial therapies.[5] Another essential metal of interest for BTSC is Zn^{II}, whose applications include Zn sensing[6,7] and anticancer activity.[8]

$^{64}Cu^{II}$ complexes of the BTSC ATSM exhibit highly interesting features such as good serum stability, small molecular weight, high cell membrane permeability and an appropriate isotope half-life (12.8 h) that make them suitable to be used as a $^{64}Cu^{II}$-based radiotracer for detecting hypoxic cells, which in turn would constitute a key point in detection of tumours.[2] This application has been proven to be especially useful in head and neck cancer.[9] Moreover, the PET imaging properties of the $^{64}Cu^{II}$ complexes with ATSM and its derivatives have also enabled the use of such systems for the detection of myocardial ischemia[10–12] and the evaluation of the development of neurodegenerative disorders such as Alzheimer's disease by targeting of amyloid-β aggregates.[13,14] In addition, further investigations are ongoing into the use of ATSM in the direct supplementation of Cu^{II} to the liver[15] as well as into the treatment of amyotrophic lateral sclerosis (ALS).[16,17] In this sense, promising results have been obtained, as can be seen from the fact that the Cu^{II}–ATSM complexes are under preclinical and clinical trials as a PET imaging agent for hypoxic lung cancer cells (phase II),[18] and as a therapeutic agent against ALS (phase II/III).[16]

All these potential applications have one common denominator: the use of Cu^{II}– or Zn^{II}–ATSM complexes in all these pathologies involves their administration *via* the blood, an aqueous medium that presents high concentrations of potential competitors for both the copper ion and the BTSC ligand. For Cu–ATSM the stability against dissociation in the serum is

[a]*ICMol, Departament de Química Inorgànica, Universitat de València, C/Catedrático José Beltrán 2, 46980 Paterna, Spain. E-mail: alvaro.martinez@uv.es*
[b]*Institut de Chimie, UMR 7177, Université de Strasbourg, CNRS, 4 Rue Blaise Pascal, 67000 Strasbourg, France*
[c]*Institut Universitaire de France (IUF), 1 rue Descartes, 75231 Paris, France*

† Electronic supplementary information (ESI) available. See DOI: https://doi.org/10.1039/d3dt02380j

well documented, but much less is known for Zn–ATSM. Another potential issue is the low solubility of Cu/Zn–ATSM complexes, which could potentially lead to precipitation.[2,14,19] The resulting complex between Cu^{II} and ATSM has an extended apolar, conjugated structure with zero net charge, which severely limits its solubility in aqueous media. On the other hand, the presence of competitors for both the Cu^{II} metal ion and the ligand ATSM in the blood could lead to dissociation or transmetallation and hence could prevent the Cu^{II}–BTSC complex from reaching its target. In this context, probably the main competitor for Cu^{II} or Zn^{II} is human serum albumin (HSA), one of the most abundant proteins in the blood (at a concentration of around 600 μM) and a key player in the distribution of essential transition metal ions in the human body, Cu^{II} and Zn^{II} among them.[20] HSA controls the distribution of copper among the internal organs and binds around 5% of Cu in blood with a relatively high affinity ($\log K_d$ ~−13 at pH 7.4); most of the remaining Cu^{II} binds strongly and inertly to ceruloplasmin (which is in turn fully loaded and therefore unable to subtract copper from Cu^{II}–ATSM).[21] HSA presents four metal ion binding sites. Of these, the coordinating centre with the highest affinity for Cu^{II} is the N-terminal site (bearing an ATCUN (amino terminal copper(II) and nickel(II)) motif).[20] HSA is also capable to coordinate Zn^{II}, constituting the main carrier of this metal ion in the human body; indeed 75–90% of Zn^{II} present in the blood is transported bound to this protein ($\log K_d$ ~7 at pH 7.4).[21] Zn^{II} is coordinated by HSA through the so-called multimetal binding site different from the main Cu^{II} N-terminal site.[22] Since ATSM and HSA are capable of coordinating both Cu^{II} and Zn^{II},[23,24] HSA could modulate the therapeutic applications of the ATSM complexes. HSA is present in the blood in its apo form as well as loaded with Cu^{II} and Zn^{II} and hence could be abstractor and source of these metal ions. Similar consideration can be made for the analogue bovine serum albumin (BSA) present in foetal calf serum often used in cell culture studies. Indeed, BSA was shown to be able to interact with Cu-complexes and change their speciation.[25]

Few of these issues have been addressed to the moment for Cu^{II}– and Zn^{II}–ATSM. Solubility seems to be still a limiting factor for physico-chemical studies of ATSM and most of its derivatives.[8] This is evidenced by the fact that up to the moment all the studies carried out with Cu^{II}–ATSM complexes have been performed in buffered media in the presence of at least 20 to 30% DMSO; otherwise, the Cu^{II} complex precipitates.[2,8,14,19] Furthermore, although the effect of reducing agents such as glutathione on the activity of Cu^{II}–ATSM complexes has been investigated,[26,27] the influence of other potential competitors such as HSA has received little attention, despite their potential impact on the effectiveness of the administration of Cu^{II}– or Zn^{II}–ATSM complexes.[2] In this sense, only a few studies regarding the influence of HSA have been reported,[2,28,29] pointing to a preference of Cu^{II}–ATSM for the IIA binding site of HSA.[28] However, these works neglect the influence of the HSA in the stability of ATSM in aqueous solutions, the transmetallation between HSA and ATSM and the combined effect on both events of multiple competitors.

In this work, we try to address both the limitations due to the low solubility and the competition between Cu^{II}, Zn^{II}, ATSM and HSA. First, we will aim to increase the solubility of both the ligand ATSM and their complexes by using the reported ATSM analogue (ATSM$(CH_2)_3$COOH) with an added carboxylic group into their structure (see Fig. 1).[30] In contrast to the water soluble ATSM developed and studied by G. Buncic, P. S. Donnelly *et al.*,[6] the alkane chain carrying the carboxylic group is expected to disturb less the conjugated system of ATSM. The idea is to introduce an additional charge into the system without modifying the coordination mode or the affinity of the ligand for Cu^{II} and Zn^{II}. Second, we will analyse the influence of the presence of equimolar concentrations of HSA and Cu^{II}/Zn^{II} on the solubility and stability of both the ligands and the complexes. Third, competition with EDTA and HSA for Cu^{II}- and Zn^{II}–ATSM/ATSM$(CH_2)_3$COOH, respectively, will permit the determination of the apparent dissociation constant at pH 7.4. All these studies will allow to deepen the understanding of the behaviour of ATSM and its Cu^{II} or Zn^{II} complexes, which could help to find new ways to improve their stability in biological media.

Experimental section

Synthesis

The synthesis of the two semicarbazone ligands ATSM and ATSM$(CH_2)_3$COOH was carried out following the procedures previously described, (see ESI section "Synthesis of the ligands"†).[1,2,30]

Methods

Computational method. The modelling of the Cu^{II} complexes was performed using the density functional theory computational method as well as the Becke three-parameter Lee–Yang–Parr hybrid functional (B3LYP).[31–33] All the gas-phase optimizations were carried out by using the Ahlrichs' basis set def2-TZV(P)[34] for all atoms except for copper, for which we employed the MDF10 Stuttgart-Dresden effective core potential.[35] The influence of the dispersion was also taken into account through Grimme's dispersion (IOp(3/124 = 30)) correction, while the effect of the polarizable solvent (water) was considered by using the default SCRF method of the polarizable continuum model.[36,37] Vibrational frequencies were computed for each minimum energy structure and, for each one of them, it was also calculated and applied the zero-point correction. Computations were carried out using the program Gaussian09 C.01,[38] while gMolden[39] and PyMOL[40] software were used for visual inspection and to create the molecular graphics.

Preparation of stock solutions. Stock solutions of Cu^{II}, HSA, HEPES, ATSM and ATSM$(CH_2)_3$COOH were prepared. The stock solution of Cu^{II} was made in Milli-Q water from the $CuCl_2{\cdot}2H_2O$ salt. The concentration of Cu^{II} was confirmed *via* direct quantification with UV-vis spectroscopy (ε_{810} = 12 M^{-1} cm^{-1})

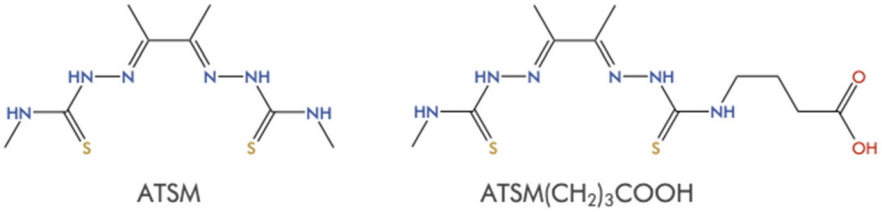

Fig. 1 Structure of ATSM and its derivative ATSM$(CH_2)_3$COOH studied in this work.

and by means of a titration with EDTA (ε_{730} = 87 M^{-1} cm^{-1}). A stock solution of HEPES buffer (50 mM, pH 7.4) was prepared dissolving free acids in Milli-Q water and adjusting the pH with NaOH. The stock solutions of ATSM and ATSM$(CH_2)_3$COOH were prepared in DMSO : HEPES (70 : 30) buffer pH 7.4 and their concentration was determined by means of titrations with Cu^{II} followed by UV-vis spectroscopy based on the well-established formation of a 1 : 1 complex.[30,41] Human serum albumin (lyophilised, essentially fatty acid free) was purchased from Sigma-Aldrich (A1887) and was dissolved in Milli-Q water. HSA concentration was first estimated *via* UV-vis spectroscopy (ε_{280} = 33 000 M^{-1} cm^{-1}).[42] However, in the present study the presence of the strong Cu^{II}-binding site is most relevant, and the N-terminus can be degraded in commercial HSA. Therefore, the here given concentration of HSA was based on the presence of the strong Cu^{II}-binding site (ATCUN). The concentration of this binding site was determined *via* a titration with Cu^{II} solution of known concentration and by following the d–d band absorption band increase around 520 nm. Stoichiometry was deduced from the halt of increase of the d–d band absorption.

UV-vis measurements. All the UV-vis titrations and kinetics were carried out in a Cary 60 spectrophotometer using a 1 cm path quartz cuvette.

Results

Solubility of the ligands

One of the main limits when working with ATSM derivatives is their stability or solubility in aqueous solutions.[2,8,14,19] Thus, before carrying out any competition study, the stability of ATSM and ATSM$(CH_2)_3$COOH in H_2O/DMSO solutions was evaluated.

First, two batch solutions containing ATSM or ATSM$(CH_2)_3$COOH at *ca.* 3 mM in 70% DMSO and 30% HEPES buffer (50 mM, pH 7.4), were prepared. Aliquots of these were taken and diluted to 30 μM in HEPES solutions containing DMSO in percentages ranging from 70% to 1%. Finally, the UV-vis spectra of the resulting solutions were recorded (see Fig. S7–S10 in the ESI†).

The solutions of the ligands in 70% of DMSO were quasi identical for ATSM and ATSM$(CH_2)_3$COOH: both compounds presented an intense band located at *ca.* 332 nm associated to the π–π* transition.[8] Moreover, their behaviour when reducing the percentage of DMSO seems to be at first sight very similar, at least for short times: the only noticeable change in the spectra is a slight hypsochromic shift (9 nm) of the absorption peaks (Fig. S7 and S8†). However, this behaviour changes when spectra are recorded over time. In the case of solutions containing ATSM in less than 30% of DMSO, a fast decrease in the intensity of the absorbance bands can be observed after a few minutes of measurement, which can be interpreted as the effect of the precipitation of the ligand (Fig. S9†). Interestingly, this behaviour is not shared with the solutions of ATSM$(CH_2)_3$COOH: their spectra stay unchanged for more than 2.5 h (Fig. S10†). This suggests that ATSM$(CH_2)_3$COOH is stable in an aqueous solution, probably thanks to the presence of the carboxylate group in its structure, which increases its net charge.

Solubility and structure of the Cu^{II} complexes

The determination of the equivalents of Cu^{II} that the ligands are capable to coordinate were determined by means of the addition of aliquots of Cu^{II} to a 30 μM solution of ATSM or ATSM$(CH_2)_3$COOH in 70% DMSO and 30% HEPES buffer (50 mM, pH 7.4). Spectra of the resulting solutions were recorded, while the intensity of the band at 470 nm was monitored to follow Cu^{II}-binding (Fig. S11 and S12†). In both cases, the intensity of the band at 470 nm stops its increase when equimolar concentration of Cu^{II} and the ligand is reached, suggesting the formation of 1 : 1 stoichiometric complexes in line with the literature for ATSM.[1,2] This observation is also in agreement with the results of the QM modelling, represented in Fig. 2. In these, indeed, the coordination takes place through a slightly distorted, square planar geometry (Houser τ_4 = 0.22).[43]

The analysis of the solubility of the Cu^{II}-L complexes followed the determination of their stoichiometry. These studies were carried out analogously to those reported in the previous section regarding the solubility of the ligands, *i.e.* by recording the absorbance spectrum of 30 μM solutions of ATSM or ATSM$(CH_2)_3$COOH, in the presence of 1 eq. of Cu^{II}, in HEPES buffer (50 mM, pH 7.4) with percentages of DMSO varying from 70 to 1% (Fig. S13–S16†).

Similar to what was observed for the ligands, the reduction in the percentage of DMSO in the medium results in a shift of the band located at *ca.* 312 nm to blue (~9 nm), and a larger hypsochromic shift (~20 nm) of the charge transfer band at around 470 to 450 nm (see Fig. S13 and S14†); without associ-

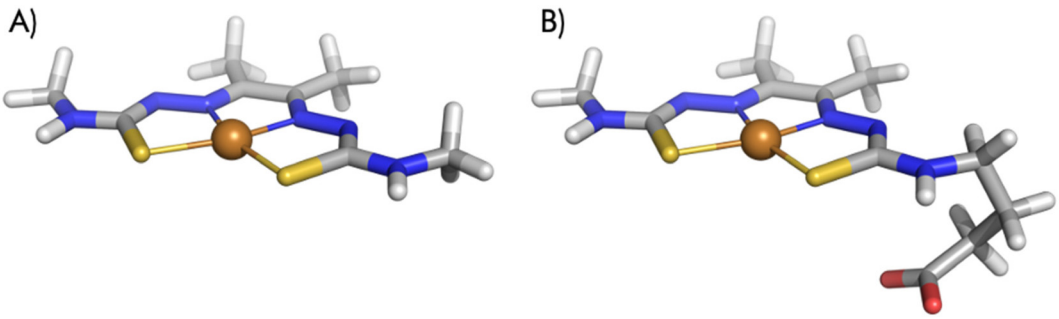

Fig. 2 Minimum energy structures of complexes (A) Cu^{II}–ATSM and (B) Cu^{II}–ATSM$(CH_2)_3$COOH obtained by geometrical optimization through QM modelling.

ated reduction of the signal intensity. But again, this effect is only valid for short measurement times since precipitation of Cu^{II}–ATSM occurs in solutions containing less than 30% of DMSO (see Fig. S15†). No variation of the signal could be observed for solutions containing Cu^{II}–ATSM$(CH_2)_3$COOH, pointing to its solubility (Fig. S16†). These results complete the observations previously reported in bibliography regarding ATSM.[2,14,19]

Competition with human serum albumin

Human serum albumin (HSA) is the highest concentrated protein in the blood (~0.6 mM) and one of the major copper binding proteins in the human organism.[21] Classically, only about 0.5% of HSA seems to be loaded with Cu^{II}.[21] HSA binds Cu^{II} in its N-terminal strong binding site with a $\log K_d \sim -13$ at pH 7.4.[44] In consequence, HSA is a potential competitor for Cu^{II}- and Zn^{II}-complexes, including Cu^{II} coordinated to ATSM or ATSM$(CH_2)_3$COOH.[22] HSA is therefore one of the main systems to be considered in the analysis of the stability of ATSM- and ATSM$(CH_2)_3$COOH-Cu^{II} complexes in biological medium.

In order to do so, two competition studies were carried out for each ligand. In the first, 1 eq. of HSA was added to a fresh solution consisting of 30 μM of ATSM (or ATSM$(CH_2)_3$COOH) and Cu^{II} (1 eq.). In the second, the opposite study was carried out, *i.e.* 1 eq. of ATSM (or ATSM$(CH_2)_3$COOH) was added to a solution containing 30 μM of HSA and 1 eq. of Cu^{II}. This approach allows to determine that the thermodynamic equilibrium is reached when the same distribution with either starting point is obtained. Spectra were collected each minute for 2.5 hours. The results are depicted in Fig. 3 and Fig. S17–S19 in ESI.†

ATSM and its carboxylic derivative ATSM$(CH_2)_3$COOH present a very similar behaviour when competing with HSA for Cu^{II}. On the one hand, albumin is not capable to take Cu^{II} when either coordinated to ATSM or ATSM$(CH_2)_3$COOH: the spectra of the complexes show no change and, in particular, no decay in the absorbance intensity of the band located at *ca.* 450 nm (charge-transfer bands of the Cu^{II} complexes, see Fig. S17 and S18†). On the other hand, when 1 equivalent of ATSM (or ATSM$(CH_2)_3$COOH) is added to a solution containing Cu^{II}–HSA, an increase of the absorbance of the band around 460 nm and a decrease of the band at *ca.* 330 nm, which corresponds to the free ligand, can be observed (Fig. 3 and S19†). From this, it can be deduced that both ligands are capable of easily subtracting the Cu^{II} coordinated to HSA. This is in agreement with the reported stability of Cu^{II}–ATSM in serum.[41,45]

But the most important observation to highlight here is that in the presence of HSA, the Cu^{II}–ATSM complex does not

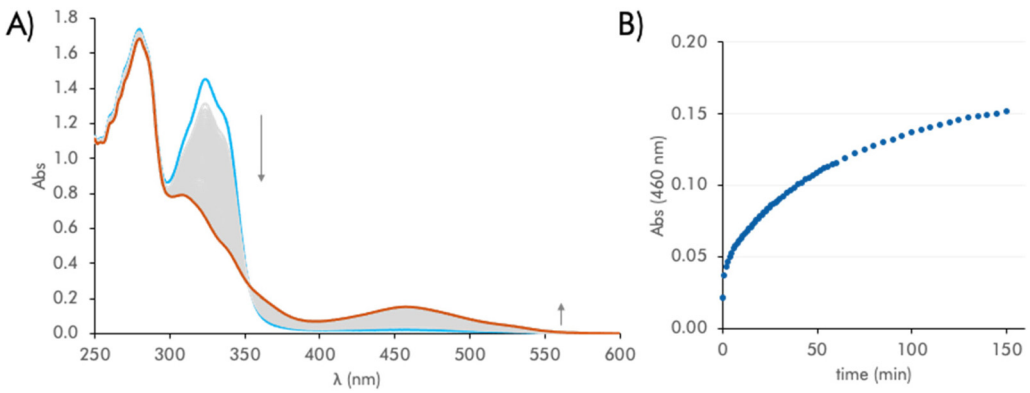

Fig. 3 (A) Evolution of the spectra with time of a 30 μM solution of Cu^{II}–HSA to which 1 eq. of ATSM was added and (B) intensity of absorbance at 460 nm as a function of time. Medium: HEPES buffer (pH 7.4, 50 mM) with 1% of DMSO.

precipitate. Contrary to what we have seen in the solubility studies, and even though the measuring medium is the same, in the presence of 1 eq. of HSA there is no reduction in the absorbance intensity of the band located above 450 nm, suggesting that albumin has a stabilising effect on this complex. In fact, the comparison between the spectra of 30 μM Cu^{II}–ATSM solutions with and without HSA shown in Fig. 4 indicates that the intensity of the charge-transfer bands is quite close in both cases, discarding the precipitation of the Cu^{II}–ATSM complex. Indeed, it can be noted that when HSA is introduced into the solution, the band at 451 nm of the Cu^{II}–ATSM complex undergoes a bathochromic shift to 459 nm. This effect is equivalent to that observed in the solubility studies, when the percentage of DMSO in solution was increased, *i.e.* when the medium had a more apolar character (see Fig. S13†). From all this, it can be deduced that the stabilisation of the complex seems to take place through its interaction with HSA, with which it is probably interacting through one of the protein binding sites, thus providing it with a more hydrophobic environment. This is in line with the studies of N. E. Basken, C. J. Mathias *et al.* in which they observed the binding of Cu–ATSM with HSA through the IIA pocket of the latter.[28,29]

The same behaviour in the spectra can be observed in the case of Cu^{II}–ATSM$(CH_2)_3$COOH. Indeed, the presence of 1 equivalent of HSA in solution leads to an even a higher red shift of the band at 452 nm (from 452 to 470 nm, see Fig. S20†). Thus, it seems that Cu^{II}–ATSM$(CH_2)_3$COOH interacts with albumin in a similar way than Cu^{II}–ATSM does, although the high solubility of the carboxylate ligand means that its interaction with the protein does not produce an additional benefit in its stabilisation in aqueous solution.

Finally, it is interesting to note that HSA is only able to stabilise ATSM when complexed to Cu^{II}. In the presence of HSA but in the absence of the metal ion, the intensity of the absorbance band of ATSM located at 323 nm decreases sharply in a similar way as it does in the absence of albumin (Fig. S21†). Thus, coordination of Cu^{II} seems to be crucial for the interaction of ATSM with HSA and therefore for keeping it soluble in aqueous media.

Competition with Zn^{II}

One of the main competitors for the thiosemicarbazone chelator in biological media is Zn^{II}, not only because of its potential affinity for the ligand but also for its relative abundance. Although HSA is the main carrier of Zn^{II} in the blood, the affinity of this metal ion for this protein is lower ($\log K_d$ ~7 at pH 7.4) than the one shown by Cu^{II}, partly due to the fact that each metal has different binding sites.[20–22] Therefore, we investigated first the competition between ATSM and HSA for Zn^{II}-binding and second the system including both metals (Cu^{II} and Zn^{II}) and both types of ligands (ATSM/ATSM$(CH_2)_3$COOH and HSA).

First, the Zn^{II}–ATSM and Zn^{II}–ATSM$(CH_2)_3$COOH complexes were characterised by recording the spectra of solutions containing 30 μM of ATSM (or ATSM$(CH_2)_3$COOH) and 1 equivalent of Zn^{II} at pH 7.4. The resulting spectra depicted in Fig. S22 and S23† show that the Zn^{II}–ATSM complexes present an intense charge-transfer band located at *ca.* 429 nm. This allows to monitor independently the formation of the Zn^{II} and the Cu^{II} complexes, thus avoiding the interferences in the measurements caused by the charge-transfer bands of the cupric complexes.

Equivalent competition studies to those carried out with Cu^{II} and HSA were implemented with Zn^{II}. To see if the HSA is capable to take Zn^{II} from the complexes, 1 equivalent of HSA was added to a 30 μM solution of Zn^{II}–ATSM (or Zn^{II}–ATSM$(CH_2)_3$COOH), and the spectrum of the resulting solution was recorded over time (Fig. S24 and S25†). The opposite competition was also carried out: 1 eq. of ATSM (or ATSM

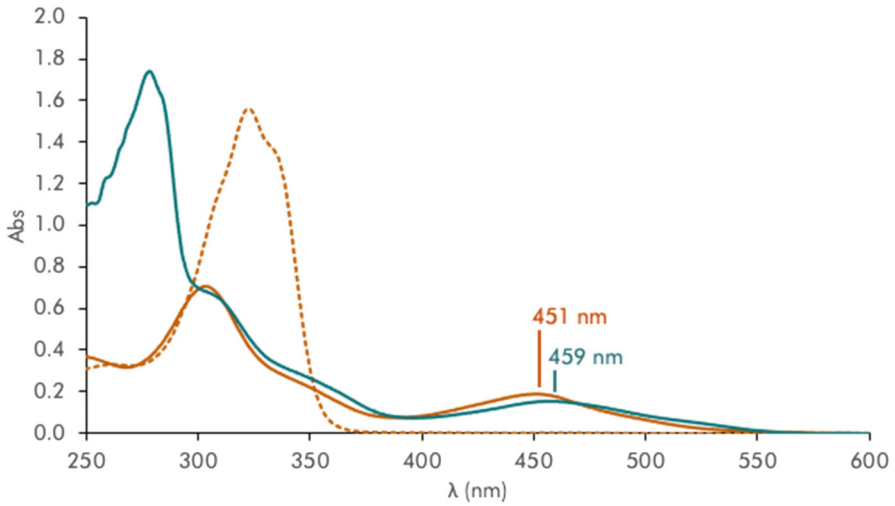

Fig. 4 Comparative of the spectra of a 30 μM ATSM solution (dotted orange line), a 30 μM ATSM solution containing 1 eq. of Cu^{II} (in dark orange) and a 30 μM ATSM solution containing 1 eq. of Cu^{II} and 1 eq. of HSA (in dark green). Medium: HEPES buffer (pH 7.4, 50 mM), 1% of DMSO.

$(CH_2)_3COOH$) was added to a solution containing 30 μM of Zn^{II}–HSA (Fig. S26 and S27†).

The main conclusion of these studies can be summarised as follows: ATSM has a similar affinity for Zn^{II} as HSA, so when HSA is added to a solution with Zn^{II}–ATSM, the protein takes up about 50% of the zinc coordinated to the bis-thiosemicarbazone, and *vice versa*. Hence the apparent binding constant at pH 7.4 for ATSM and ATSM$(CH_2)_3$COOH, $\log K^{app}_{pH7.4}$ is about −7. As shown in Fig. 5, the addition of ATSM to a solution containing Zn^{II}–HSA produces a decay in the band located at *ca.* 330 nm and an increase of the band at 408 nm, processes that are correlated with the formation of the Zn^{II}–ATSM complexes. In other words, ATSM is capable to take Zn^{II} from HSA. But, interestingly, the uptake of Zn^{II} is not complete, but ends when about half of the available zinc has been taken up. This can be clearly observed when a second Zn^{II} equivalent is added to the solution: the absorbance of the band at 408 nm increases from *ca.* 0.1 to 0.2, suggesting that about half of the ATSM was not coordinating Zn^{II}. These conclusions are reproduced for the reverse competition studies: when 1 eq. of HSA is added to a Zn^{II}–ATSM solution, a rapid increase of the band at 330 nm can be observed, together with the decrease of the band at 408 nm, which translates into a significant loss of Zn^{II} from the ATSM. More importantly, the trends of both competitions converge to the same absorbance value (*ca.* 0.1), suggesting that an equilibrium is reached (see Fig. 5B). The studies carried out with ATSM$(CH_2)_3$COOH lead to the same conclusions, pointing to a very similar behaviour of this ligand to the one found for ATSM (see Fig. S25, S26 and S28†).

Regarding the stability of the Zn^{II}–ATSM complexes, it is worth mentioning that similarly to the Cu^{II} complexes, also in this case HSA exerts a stabilising effect on the Zn^{II} compounds, avoiding precipitation, as can be seen in Fig. 5B.

Once studied the coordination of Zn^{II} by the bis-thiosemicarbazone ligands, the effect of this competitor over the Cu^{II} complexes was analysed. This was carried out by recording the spectra of solutions of Cu^{II}–ATSM (or Cu^{II}–ATSM$(CH_2)_3$COOH) (30 μM) after the addition of 0.1 to 100 equivalents of Zn^{II}. No changes can be observed in the spectra of the Cu^{II} complexes after the addition of any of these amounts of Zn^{II} (see Fig. S29 and S30†), which implies that the Cu^{II} complexes are robust enough to prevent the exchange of the metal ion even in presence of 100 equivalents of Zn^{II}, as it was expected from reports in the literature of Zn and Cu^{II}–ATSM stability,[24] although done with high amounts of DMSO.

In order to explore the combined effect of HSA and Zn^{II}, 1 eq. of HSA and 10 eq. of Zn^{II} were added to a solution containing 30 μM of Cu^{II}–ATSM (or Cu^{II}–ATSM$(CH_2)_3$COOH), and then the spectra of the resulting solutions were recorded over time. In this case, the two competitors with different but complementary targets were combined: HSA for its affinity for Cu^{II}, and Zn^{II} for its affinity for the ATSM derivatives. As depicted in Fig. 6 and S31,† both Cu^{II}–ATSM and Cu^{II}–ATSM$(CH_2)_3$COOH can resist the combined presence of HSA and 10 eq. of Zn^{II}.

Finally, one last question remains to be solved: what happens when the nude bis-thiosemicarbazone is added to a solution containing HSA, Cu^{II} and Zn^{II}? As mentioned, HSA is capable to coordinate both metal ions at the same time, the Cu^{II} through the ATCUN motive and the Zn^{II} by means of the multi-metal binding site.[20] Thus, in this case the competition with ATSM or ATSM$(CH_2)_3$COOH will be influenced not only by the presence of the different metal ions, but also by the relative stability given by each chelating site and the kinetics of the exchange. This matter was explored by recording the absorbance spectrum over time of a 30 μM solution of Cu^{II}–Zn^{II}–HSA after the addition of 1 eq. of ATSM or ATSM$(CH_2)_3$COOH. The results of this competitions are depicted in Fig. 7, 8 and S32–S34.†

The main conclusion of the studies carried out is that the bis-thiosemicarbazone ligands examined have a clear kinetic preference for Zn^{II}, the latter being the first to be captured from HSA already during mixing time, whereas Cu^{II} complexes

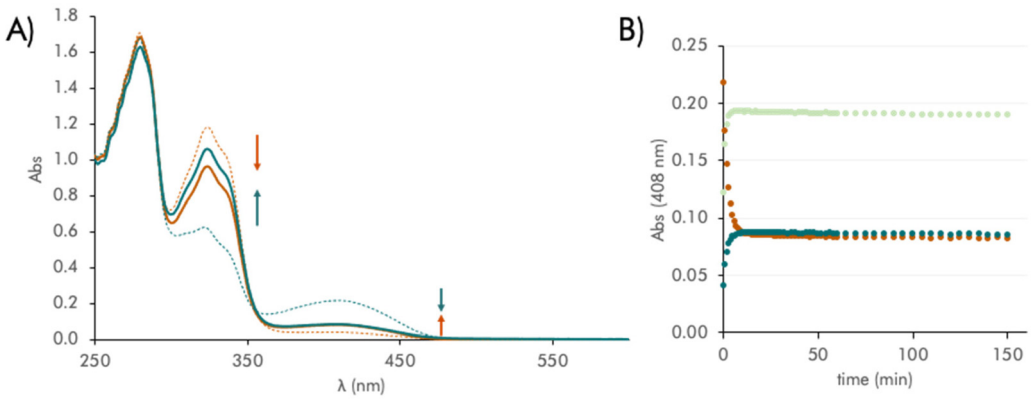

Fig. 5 (A) Comparison between the addition of HSA to a solution of Zn^{II}–ATSM (in orange) and the addition of ATSM to a solution of Zn^{II}–HSA (in green), [ATSM] = [HSA] = [Zn^{II}] = 30 μM, dotted lines correspond to spectra at time 0, and continuous lines correspond to spectra at time 150 min. (B) Intensity of absorbance at 408 nm for the addition of HSA to a solution of Zn^{II}–ATSM (in orange), the addition of ATSM to a solution of Zn^{II}–HSA (1 : 1) (in dark green) and the addition of ATSM to a solution of Zn^{II}–HSA (2 : 1) (in pale green). Medium: HEPES buffer (pH 7.4, 50 mM) with 1% of DMSO.

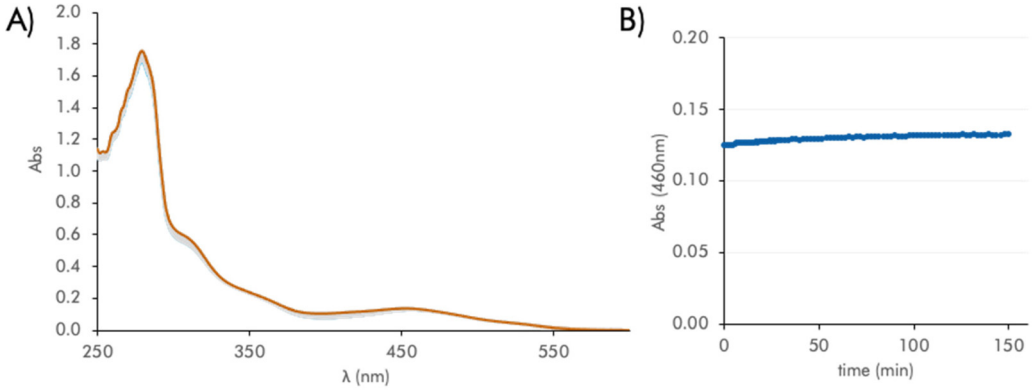

Fig. 6 (A) Evolution of the spectra with time of a 30 μM solution of Cu^{II}–ATSM after the addition of 1 eq. of HSA and 10 eq. of Zn^{II}, (B) intensity of absorbance at 460 nm as a function of time. Medium: HEPES buffer (pH 7.4, 50 mM) with 1% of DMSO.

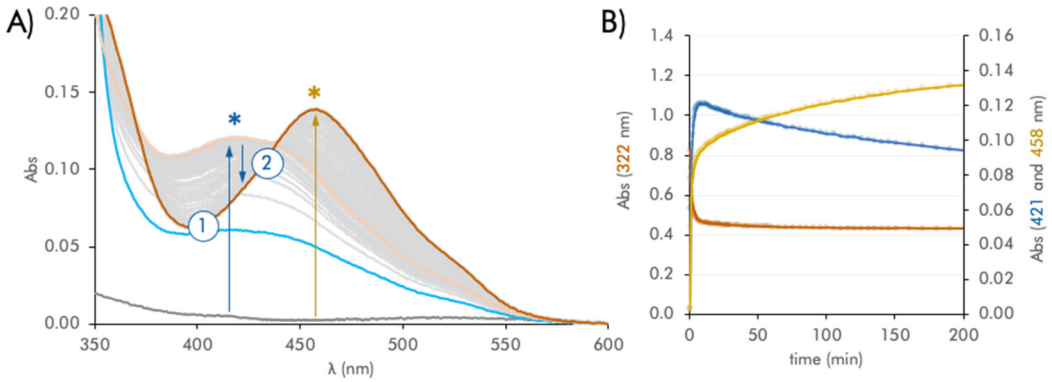

Fig. 7 (A) Detail of the evolution of the spectra with time of a 30 μM solution of Cu^{II}–Zn^{II}–HSA after the addition of 1 eq. of ATSM, (B) intensity of absorbance of the ligand (322 nm, orange), the Zn^{II} complex (421 nm, blue) and the Cu^{II} complex (458 nm, yellow) as a function of time. Medium: HEPES buffer (pH 7.4, 50 mM) with 1% of DMSO.

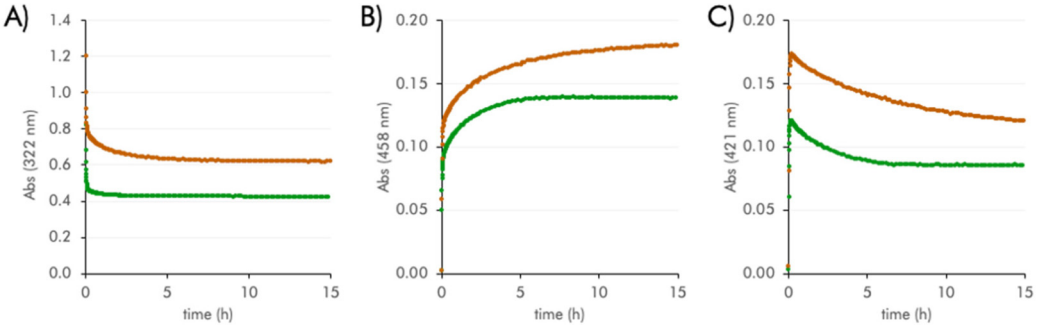

Fig. 8 Comparative of the evolution of the bands corresponding to (A) the ligand, (B) the Cu^{II} complexes and (C) the Zn^{II} complexes after the addition of 1 eq. of ATSM (green) and ATSM$(CH_2)_3$COOH (orange) to a 30 μM solution of Cu^{II}–Zn^{II}–HSA. Medium: HEPES buffer (pH 7.4, 50 mM) with 1% of DMSO.

are thermodynamically more stable, so that after a few minutes a slow transmetallation of Zn^{II} by Cu^{II} takes place. This transmetallation is quite slow and lasts several hours. These observations are valid both for ATSM and ATSM$(CH_2)_3$COOH, so we will focus on the performance of the former to analyse these kinetics (Fig. 7 and S32†). First, after the addition of 1 eq. of ATSM to the solution containing Cu^{II}–Zn^{II}–HSA, the absorbance of the band corresponding to the Zn^{II} complexes (421 nm) rapidly increases, reaching its maximum at *ca.* 10 min after addition. At the same time, the band of the π–π* transitions of the ligand sharply decreases. Both processes are correlated with the formation of the

Zn^{II}–ATSM complexes and, indeed, the profile of the band at 421 nm is quite clear, discarding the early coordination of Cu^{II}. Therefore, the Zn^{II} complexes are kinetically favoured, so Zn^{II} is the first metal to be taken from HSA.

After *ca.* 10 min, the tendency shown by the spectra changes. The band of the Zn^{II}–ATSM complex (421 nm) stops its increase and starts to slowly decrease in intensity while, at the same time, the absorbance band of the Cu^{II}–ATSM complex (458 nm) steadily increases. This behaviour points to a substitution of Zn^{II} by Cu^{II} in the ATSM complexes. Moreover, after the initial fast decrease of the band at 322 nm (that corresponds to the ligand), this band does not show any change in profile or intensity, even as the bands of the Cu^{II} and Zn^{II} complexes continue to change (Fig. 7B). This suggests that the total concentration of complexes remains constant, which supports the idea that the changes in the bands at 421 and 458 nm are due to transmetallation.

In short, although the capture of Zn^{II} from HSA is kinetically favoured, the Cu^{II}–ATSM complexes are more stable in thermodynamic terms. Thus, Zn^{II}–ATSM complexes are initially formed, Zn^{II} is slowly replaced by Cu^{II}. In fact, the final spectrum suggests that transmetallation has been complete and Cu^{II} has been able to completely replace Zn^{II} in the ATSM complexes.

The behaviour of ATSM$(CH_2)_3$COOH is very similar to the one shown by ATSM, presenting the same tendencies, rapid binding of Zn^{II} followed by slow transmetallation by Cu^{II} (Fig. S33 and S34†). However, there are a few points in which ATSM and ATSM$(CH_2)_3$COOH differ. As shown in the trends of the π–π* bands of the ligands and the charge transfer ones of the Cu^{II} and Zn^{II} complexes (322, 458 and 421 nm, respectively, Fig. 8), the two main differences between both ligands were: (A) the final intensity of the bands that imply ATSM are always lower than those corresponding to ATSM$(CH_2)_3$COOH and (B) the kinetics involving ATSM$(CH_2)_3$COOH were slower. Both behaviours can be explained by the limited solubility of ATSM. The lower intensity of the bands of Cu^{II}– and Zn^{II}–ATSM complexes compared with ATSM$(CH_2)_3$COOH would imply a higher concentration of uncoordinated ATSM, but this is not the case: the intensity of the band at 322 is also lower for ATSM. The limited solubility of this ligand in water leads to its precipitation and, thus, to the reduction of its capacity of taking Cu^{II} or Zn^{II} from HSA. This precipitation of ATSM alone during the reaction could also explain the apparent faster kinetics of Cu^{II} transfer from HSA to ATSM than (ATSM$(CH_2)_3$COOH).

Competition with EDTA

The next competitor for Cu^{II} analysed in the work was ethylenediaminetetraacetic acid (EDTA), a hexadentate chelator with well-known affinities for many metal ions including Cu^{II}, for which EDTA presents an apparent formation constant of 15.9 at pH 7.4 logarithmic units.[22,46]

Equivalent competition assays to those implemented previously were carried out for the study of the capacity of EDTA to take Cu^{II} from the Cu^{II}–ATSM and Cu^{II}–ATSM$(CH_2)_3$COOH complexes (Fig. S35–S40†): for this, the absorbance spectra of solutions containing 30 μM of ATSM (or ATSM$(CH_2)_3$COOH) and 1 equivalent of EDTA at pH 7.4 was recorded over time (Fig. S35 and S36†).

As expected, the Cu^{II}–ATSM rapidly precipitates in solution, as previously observed in the absence of EDTA, but this process is not associated with (nor stimulated by) any transfer of Cu^{II} to EDTA. As can be seen in Fig. S35,† the decay in absorbance intensity takes place in a similar proportion for the bands located around 330 and 450 nm. In the case of a hypothetical Cu^{II} transfer from ATSM to EDTA, the band at 330 nm should increase in intensity (or at least decay at a lower rate) than the one located at 450 nm. Moreover, when the complex is completely solubilised in solution, *i.e.* when we have a percentage of DMSO higher than 20% or there is 1 equivalent of HSA in solution, no alteration in the absorbance bands is observed (Fig. S35†), which confirms the observation of the failure of EDTA to take up Cu^{II} from ATSM. Equivalent results are obtained when studying ATSM$(CH_2)_3$COOH (Fig. S36†) instead of ATSM: even with measurement times exceeding 500 h, no modification of the spectrum is observed, confirming the hypothesis of null Cu^{II} transfer from these thiosemicarbazone ligands to EDTA.

To rule out kinetic factors as the cause of the reduced Cu^{II} transfer, this competition was also set up in reverse: 1 eq. of ATSM (or ATSM$(CH_2)_3$COOH) was added to a solution containing 30 μM of Cu^{II}–EDTA (in the case of ATSM, 1 eq. of HSA was also added to the solution in order to stabilise the resulting Cu^{II}–ATSM complexes). The results are depicted in Fig. 9 and S38.† When the measurement is carried out with ATSM, a clear decrease in the intensity of the absorbance band at 330 nm associated with the ligand is observed (Fig. S38†). Since this change is not followed by an increase in the intensity of the band above 450 nm, which would correspond to the formation of the Cu^{II}–ATSM complex, we can deduce that it is rather related to the precipitation of the ligand. This seems to occur fast enough to prevent the ligand from being able to take up the Cu^{II} from the Cu^{II}–EDTA, since HSA is not capable to stabilise ATSM in its non-metalated form, as previously shown. These observations are confirmed when moving on to study ATSM$(CH_2)_3$COOH (see Fig. 9).

As previously shown, ATSM$(CH_2)_3$COOH is soluble in aqueous media. Therefore, although the intensity of the band of ATSM$(CH_2)_3$COOH located around 330 nm also decreases with time, this is not related to the precipitation of the ligand but to the transfer of Cu^{II} from the EDTA ligand to ATSM$(CH_2)_3$COOH and to the formation of the corresponding Cu^{II}–ATSM$(CH_2)_3$COOH complex. This is confirmed by the appearance of the band at 450 nm. From this study it can also be deduced that the affinity constant of ATSM$(CH_2)_3$COOH for Cu^{II} must be considerably greater than the one of EDTA.

In order to explore this aspect in more depth and to determine the thermodynamic apparent complexation constant of Cu^{II} with these thiosemicarbazone ligands at pH 7.4, the previous assessments were repeated increasing the equivalents of EDTA employed from 1 to 1000 (Fig. 10 and S39, S40†). Due to

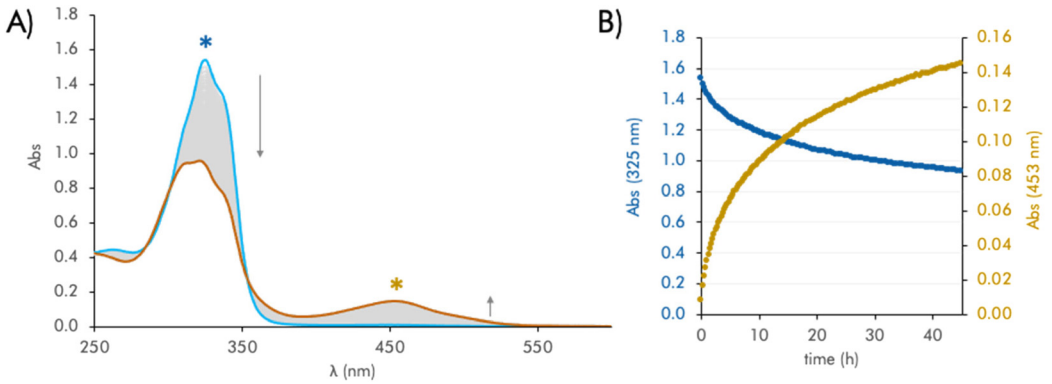

Fig. 9 (A) Evolution of the spectra with time of a 30 μM solution of Cu^{II}–EDTA after the addition of 1 eq. of ATSM$(CH_2)_3$COOH, (B) intensity of absorbance at 325 nm (in blue) and at 453 nm (in yellow) as a function of time. Medium: HEPES buffer (pH 7.4, 50 mM) with 1% of DMSO.

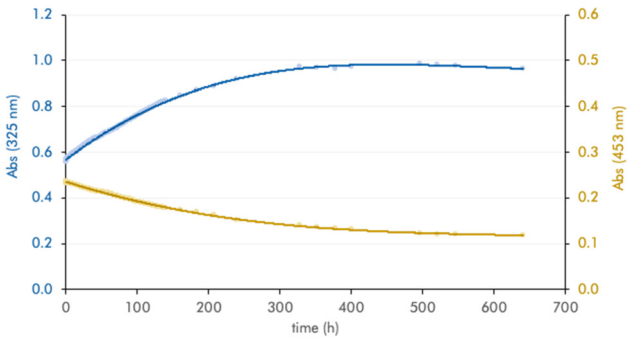

Fig. 10 Intensity of absorbance at 325 nm (in blue) and 453 nm (in yellow) as a function of time when 1000 eq. of EDTA were added to a 30 μM solution of Cu^{II}–ATSM$(CH_2)_3$COOH measured for 650 h. Medium: HEPES buffer (pH 7.4, 50 mM) with 1% of DMSO.

the solubility issues of ATSM, these studies were only implemented with ATSM$(CH_2)_3$COOH. When 1 eq. of ATSM $(CH_2)_3$COOH is added to a 30 μM solution of Cu^{II} and 1000 eq. of EDTA, it can be observed that the thiosemicarbazone is still able to take Cu^{II} from Cu^{II}–EDTA (Fig. S39†). Moreover, if the opposite competition is carried out, *i.e.* when 1000 equivalents of EDTA are added over a 30 μM solution of Cu^{II}–ATSM $(CH_2)_3$COOH, a very slow demetallation of the latter complex can be observed (Fig. S40†). Once equilibrium is reached (after more than 600 h of kinetics, Fig. 10), 50% of ATSM $(CH_2)_3$COOH is demetallated, which suggests that the apparent complexation constant of Cu^{II}–ATSM$(CH_2)_3$COOH is *ca.* three orders of magnitude higher than the one of Cu^{II}–EDTA, *i.e.* ~18.9 logarithmic units at pH 7.4.[22,46] This value is in agreement with the log K_d of −18.2 for PTSM, the analogue of ATSM with a H instead of a Me on one of the central carbons.[47]

Conclusions

Two major properties regarding ATSM have been addressed in this work, the solubility of its Cu^{II} complexes and their stability against potential competitors such as HSA and Zn^{II}. The introduction of a propyl carboxylic group in the ATSM structure has made possible to solubilise both the ligand and the Cu^{II} or Zn^{II} complexes in solutions containing less than 1% DMSO without altering the coordination mode and the conjugated system of the ligand. In addition, we confirm the observed stability of Cu^{II} complexes with ATSM in serum-like conditions: ATSM and ATSM$(CH_2)_3$COOH Cu^{II} complexes are stable in the presence of the biologically relevant competitors, HSA and Zn^{II}, even when acting in combination and in close to biological proportions. The competition assays for Cu^{II} of EDTA with the water soluble ATSM$(CH_2)_3$COOH yielded an apparent log K_d at pH 7.4 of about −18.9. A similar value could be expected for ATSM. In addition, Cu^{II}–ATSM most likely forms a ternary complex with HSA, which is presumably the reason why this protein prevents the precipitation of these ATSM complexes in aqueous solution. Such binding of Cu^{II}–ATSM to HSA could also occur in the blood and could not only avoid precipitation, but also aiding the distribution of Cu^{II}–ATSM throughout the organism impacting its biodistribution and pharmacokinetics. Furthermore, given the ability of ATSM derivatives to subtract Cu^{II} from HSA, this protein could be considered as a potential source of Cu^{II} for ATSM$(CH_2)_3$COOH or ATSM, although limited by the low Cu^{II} content of HSA and the slow transfer (min to h) of Cu^{II} from HSA to ATSM. On the other hand, ATSM and HSA present similar affinities for Zn^{II}, hence an apparent log K_d at pH 7.4 of about −7 can be deduced. These results open up interesting possibilities for further research. Hence, Zn^{II}–ATSM risks to loose at least part of its Zn^{II} to the highly concentrated apo-HSA quite fast, and moreover, is expected to pick up the Cu^{II} from HSA. Hence a partial transmetallation could be expected, but with a very slow kinetics (min to hours). Administration of the ligand ATSM alone, could lead to the partial formation of Zn^{II}–ATSM, which could be kinetically stable for a longer time even in the presence of Cu^{II}-bound to HSA. Taken together, the here reported multifaceted interactions between ATSM, HSA, Cu^{II} and Zn^{II} might help to better understand the behaviour of ATSM and its Cu^{II} and Zn^{II} complexes *in vivo*.

Conflicts of interest

There are no conflicts of interest to declare.

Acknowledgements

We would like to thank all the members of the BCB group at the Institut de Chimie de Strasbourg (UMR 7177) for fruitful discussion on the topic, and in particular K. Zimmeter for providing HSA solutions. A. M.-C. wants to acknowledge the support received under the "Margarita Salas" post-doctoral program (grant MS21-095) funded by the Ministerio de Universidades from the Spanish Government and the European Union – NextGenerationEU.

References

1 C. Stefani, Z. Al-Eisawi, P. J. Jansson, D. S. Kalinowski and D. R. Richardson, *J. Inorg. Biochem.*, 2015, **152**, 20–37.
2 G. R. Walke and S. Ruthstein, *ACS Omega*, 2019, **4**, 12278–12285.
3 D. Xie, S. Kim, V. Kohli, A. Banerjee, M. Yu, J. S. Enriquez, J. J. Luci and E. L. Que, *Inorg. Chem.*, 2017, **56**, 6429–6437.
4 D. Palanimuthu, S. V. Shinde, K. Somasundaram and A. G. Samuelson, *J. Med. Chem.*, 2013, **56**, 722–734.
5 K. Bajaj, R. M. Buchanan and C. A. Grapperhaus, *J. Inorg. Biochem.*, 2021, **225**, 111620.
6 G. Buncic, P. S. Donnelly, B. M. Paterson, J. M. White, M. Zimmermann, Z. Xiao and A. G. Wedd, *Inorg. Chem.*, 2010, **49**, 3071–3073.
7 D. Dayal, D. Palanimuthu, S. V. Shinde, K. Somasundaram and A. G. Samuelson, *JBIC, J. Biol. Inorg. Chem.*, 2011, **16**, 621–632.
8 R. Anjum, D. Palanimuthu, D. S. Kalinowski, W. Lewis, K. C. Park, Z. Kovacevic, I. U. Khan and D. R. Richardson, *Inorg. Chem.*, 2019, **58**, 13709–13723.
9 I. Grassi, C. Nanni, G. Cicoria, C. Blasi, F. Bunkheila, E. Lopci, P. M. Colletti, D. Rubello and S. Fanti, *Clin. Nucl. Med.*, 2014, **39**, e59–e63.
10 B. M. Paterson, C. Cullinane, P. J. Crouch, A. R. White, K. J. Barnham, P. D. Roselt, W. Noonan, D. Binns, R. J. Hicks and P. S. Donnelly, *Inorg. Chem.*, 2019, **58**, 4540–4552.
11 A. L. Vävere and J. S. Lewis, *Dalton Trans.*, 2007, 4893.
12 M. G. Handley, R. A. Medina, E. Nagel, P. J. Blower and R. Southworth, *J. Mol. Cell. Cardiol.*, 2011, **51**, 640–650.
13 J. L. Hickey, S. Lim, D. J. Hayne, B. M. Paterson, J. M. White, V. L. Villemagne, P. Roselt, D. Binns, C. Cullinane, C. M. Jeffery, R. I. Price, K. J. Barnham and P. S. Donnelly, *J. Am. Chem. Soc.*, 2013, **135**, 16120–16132.
14 A. Noor, D. J. Hayne, S. Lim, J. K. Van Zuylekom, C. Cullinane, P. D. Roselt, C. A. McLean, J. M. White and P. S. Donnelly, *Inorg. Chem.*, 2020, **59**, 11658–11669.
15 T. A. Su, D. S. Shihadih, W. Cao, T. C. Detomasi, M. C. Heffern, S. Jia, A. Stahl and C. J. Chang, *J. Am. Chem. Soc.*, 2018, **140**, 13764–13774.
16 S. Nikseresht, J. B. W. Hilton, K. Kysenius, J. R. Liddell and P. J. Crouch, *Life*, 2020, **10**, 1–14.
17 B. G. Trist, J. B. Hilton, D. J. Hare, P. J. Crouch and K. L. Double, *Angew. Chem., Int. Ed.*, 2021, **60**, 9215–9246.
18 A. Challapalli, L. Carroll and E. O. Aboagye, *Clin. Transl. Imaging*, 2017, **5**, 225–253.
19 J. L. J. Dearling, J. S. Lewis, G. E. D. Mullen, M. J. Welch and P. J. Blower, *JBIC, J. Biol. Inorg. Chem.*, 2002, **7**, 249–259.
20 W. Bal, M. Sokołowska, E. Kurowska and P. Faller, *Biochim. Biophys. Acta, Gen. Subj.*, 2013, **1830**, 5444–5455.
21 E. Falcone and P. Faller, *Dalton Trans.*, 2023, **52**, 2197–2208.
22 T. Kirsipuu, A. Zadorožnaja, J. Smirnova, M. Friedemann, T. Plitz, V. Tõugu and P. Palumaa, *Sci. Rep.*, 2020, **10**, 5686.
23 M. Christlieb, J. P. Holland and J. R. Dilworth, *Inorg. Chim. Acta*, 2010, **363**, 1133–1139.
24 E. J. McAllum, B. R. Roberts, J. L. Hickey, T. N. Dang, A. Grubman, P. S. Donnelly, J. R. Liddell, A. R. White and P. J. Crouch, *Neurobiol. Dis.*, 2015, **81**, 20–24.
25 P. Nunes, I. Correia, F. Marques, A. P. Matos, M. M. C. dos Santos, C. G. Azevedo, J.-L. Capelo, H. M. Santos, S. Gama, T. Pinheiro, I. Cavaco and J. C. Pessoa, *Inorg. Chem.*, 2020, **59**, 9116–9134.
26 F. Shaughnessy, E. Mariotti, K. P. Shaw, T. R. Eykyn, P. J. Blower, R. Siow and R. Southworth, *EJNMMI Res.*, 2014, **4**, 40.
27 J. M. Floberg, L. Wang, N. Bandara, R. Rashmi, C. Mpoy, J. R. Garbow, B. E. Rogers, G. J. Patti and J. K. Schwarz, *J. Nucl. Med.*, 2020, **61**, 427–432.
28 N. E. Basken, C. J. Mathias and M. A. Green, *J. Pharm. Sci.*, 2009, **98**, 2170–2179.
29 N. E. Basken, C. J. Mathias, A. E. Lipka and M. A. Green, *Nucl. Med. Biol.*, 2008, **35**, 281–286.
30 B. M. Paterson, J. A. Karas, D. B. Scanlon, J. M. White and P. S. Donnelly, *Inorg. Chem.*, 2010, **49**, 1884–1893.
31 J. P. Perdew, *Phys. Rev. B: Condens. Matter Mater. Phys.*, 1986, **33**, 8822–8824.
32 A. D. Becke, *Phys. Rev. A*, 1988, **38**, 3098–3100.
33 C. Lee, W. Yang and R. G. Parr, *Phys. Rev. B: Condens. Matter Mater. Phys.*, 1988, **37**, 785–789.
34 F. Weigend and R. Ahlrichs, *Phys. Chem. Chem. Phys.*, 2005, **7**, 3297–3305.
35 D. Andrae, U. Häußermann, M. Dolg, H. Stoll and H. Preuß, *Theor. Chim. Acta*, 1990, **77**, 123–141.
36 S. Grimme, J. Antony, S. Ehrlich and H. Krieg, *J. Chem. Phys.*, 2010, **132**, 154104.
37 J. Tomasi, B. Mennucci and R. Cammi, *Chem. Rev.*, 2005, **105**, 2999–3093.
38 M. J. Frisch, G. W. Trucks, H. B. Schlegel, G. E. Scuseria, M. A. Robb, J. R. Cheeseman, G. Scalmani, V. Barone, B. Mennucci, G. A. Petersson, H. Nakatsuji, M. Caricato, X. Li, H. P. Hratchian, A. F. Izmaylov, J. Bloino, G. Zheng,

J. L. Sonnenberg, M. Hada, M. Ehara, K. Toyota, R. Fukuda, J. Hasegawa, M. Ishida, T. Nakajima, Y. Honda, O. Kitao, H. Nakai, T. Vreven, J. A. Montgomery Jr., J. E. Peralta, F. Ogliaro, M. Bearpark, J. J. Heyd, E. Brothers, K. N. Kudin, V. N. Staroverov, T. Keith, R. Kobayashi, J. Normand, K. Raghavachari, A. Rendell, J. C. Burant, S. S. Iyengar, J. Tomasi, M. Cossi, N. Rega, J. M. Millam, M. Klene, J. E. Knox, J. B. Cross, V. Bakken, C. Adamo, J. Jaramillo, R. Gomperts, R. E. Stratmann, O. Yazyev, A. J. Austin, R. Cammi, C. Pomelli, J. W. Ochterski, R. L. Martin, K. Morokuma, V. G. Zakrzewski, G. A. Voth, P. Salvador, J. J. Dannenberg, S. Dapprich, A. D. Daniels, O. Farkas, J. B. Foresman, J. V. Ortiz, J. Cioslowski and D. J. Fox, 2009.

39 G. Schaftenaar and J. H. Noordik, *J. Comput.-Aided Mol. Des.*, 2000, **14**, 123–134.

40 The PyMOL Molecular Graphics System, Version 1.7.7.2 Schrödinger, LLC 2015.

41 A. R. Cowley, J. R. Dilworth, P. S. Donnelly, J. M. Heslop and S. J. Ratcliffe, *Dalton Trans.*, 2007, 209–217.

42 E. Stefaniak, D. Płonka, S. C. Drew, K. Bossak-Ahmad, K. L. Haas, M. J. Pushie, P. Faller, N. E. Wezynfeld and W. Bal, *Metallomics*, 2018, **10**, 1723–1727.

43 L. Yang, D. R. Powell and R. P. Houser, *Dalton Trans.*, 2007, 955–964.

44 K. Bossak-Ahmad, T. Frączyk, W. Bal and S. C. Drew, *ChemBioChem*, 2020, **21**, 331–334.

45 R. Hueting, V. Kersemans, B. Cornelissen, M. Tredwell, K. Hussien, M. Christlieb, A. D. Gee, J. Passchier, S. C. Smart, J. R. Dilworth, V. Gouverneur and R. J. Muschel, *J. Nucl. Med.*, 2014, **55**, 128–134.

46 C. S. Atwood, R. C. Scarpa, X. Huang, R. D. Moir, W. D. Jones, D. P. Fairlie, R. E. Tanzi and A. I. Bush, *J. Neurochem.*, 2000, **75**, 1219–1233.

47 D. A. Winkelmann, Y. Bermke and D. H. Petering, *Bioinorg. Chem.*, 1974, **3**, 261–277.